Biochem. J. (1990) 271, 515–522 (Printed in Great Britain)

SK&F 96365, a novel inhibitor of receptor-mediated calcium entry

Janet E. MERRITT,* W. Paul ARMSTRONG,† Christopher D. BENHAM, Trevor J. HALLAM,‡ Ron JACOB, Albert JAXA-CHAMIEC,‡ Beatrice K. LEIGH, Sean A. McCARTHY, Kitty E. MOORES and Timothy J. RINK§

SmithKline Beecham Pharmaceuticals, The Frythe, Welwyn, Herts. AL6 9AR, U.K.

A novel inhibitor of receptor-mediated calcium entry (RMCE) is described. SK&F 96365 (1-{β-[3-(4-methoxyphenyl)propoxy]-4-methoxyphenethyl}-1*H*-imidazole hydrochloride) is structurally distinct from the known 'calcium antagonists' and shows selectivity in blocking RMCE compared with receptor-mediated internal Ca^{2+} release. Human platelets, neutrophils and endothelial cells were loaded with the fluorescent Ca^{2+}-indicator dyes quin2 or fura-2, in order to measure Ca^{2+} or Mn^{2+} entry through RMCE as well as Ca^{2+} release from internal stores. The IC_{50} (concn. producing 50% inhibition) for inhibition of RMCE by SK&F 96365 in platelets stimulated with ADP or thrombin was 8.5 μM or 11.7 μM respectively; these concentrations of SK&F 96365 did not affect internal Ca^{2+} release. Similar effects of SK&F 96365 were observed in suspensions of neutrophils and in single endothelial cells. SK&F 96365 also inhibited agonist-stimulated Mn^{2+} entry in platelets and neutrophils. The effects of SK&F 96365 were independent of cell type and of agonist, as would be expected for a compound that modulates post-receptor events. Voltage-gated Ca^{2+} entry in fura-2-loaded GH_3 (pituitary) cells and rabbit ear-artery smooth-muscle cells held under voltage-clamp was also inhibited by SK&F 96365; however, the ATP-gated Ca^{2+}-permeable channel of rabbit ear-artery smooth-muscle cells was unaffected by SK&F 96365. Thus SK&F 96365 (unlike the 'organic Ca^{2+} antagonists') shows no selectivity between voltage-gated Ca^{2+} entry and RMCE, although the lack of effect on ATP-gated channels indicates that it discriminates between different types of RMCE. The effects of SK&F 96365 on functional responses of cells thought to be dependent on Ca^{2+} entry via RMCE were also studied. Under conditions where platelet aggregation is dependent on stimulated Ca^{2+} entry via RMCE, the response was blocked by SK&F 96365 with an IC_{50} of 15.9 μM, which is similar to the IC_{50} of 8–12 μM observed for inhibition of RMCE. Adhesion and chemotaxis of neutrophils were also inhibited by SK&F 96365. SK&F 96365 is a useful tool to distinguish RMCE from internal Ca^{2+} release, and to probe the role of RMCE in mediating functional responses of cells. However, SK&F 96365 is not as potent (IC_{50} around 10 μM) or selective (also inhibits voltage-gated Ca^{2+} entry) as would be desirable, so caution must be exercised when using this compound.

INTRODUCTION

In view of its central importance, it is not surprising that multiple mechanisms have evolved for the stimulus-evoked transfer of Ca^{2+} into the cytosol. Considerable progress has been made in elucidating two of these mechanisms: the intracellular release evoked by $InsP_3$ (Berridge, 1988; Putney, 1987) and the entry of Ca^{2+} via voltage-gated calcium channels (Campbell *et al.*, 1988; Tsien *et al.*, 1988). This progress has been greatly helped by the availability of high-affinity ligands, including $InsP_3$ itself (Ross *et al.*, 1989), and the organic 'calcium antagonists' and toxins for voltage-gated channels (Campbell *et al.*, 1988; Tsien *et al.*, 1988). It has proved harder to elucidate the mechanisms and function of a third general class of Ca^{2+}-mobilizing mechanisms, receptor-mediated Ca^{2+} entry (RMCE). There have been recent advances in establishing the existence and diversity of RMCE (Meldolesi & Pozzan, 1987; Hallam & Rink, 1989), mainly in non-excitable cells, but electrophysiological studies have proved difficult, and a serious impediment is the lack of suitable ligands. We report here investigations of RMCE in human platelets, neutrophils and endothelial cells, using a novel compound, SK&F 96365, which is structurally distinct from classic calcium antagonists and which shows selectivity in blocking RMCE compared with internal Ca^{2+} release.

Effects of SK&F 96365 on agonist-stimulated Ca^{2+} entry in these cells were assessed by measuring fluorescence signals from intracellular quin2 or fura-2 (Cobbold & Rink, 1987; Grynkiewicz *et al.*, 1985). Effects on bivalent cation entry were also monitored by using Mn^{2+} as a surrogate for Ca^{2+} (Hallam & Rink, 1985; Merritt *et al.*, 1989*a*). The influence of SK&F 96365 on voltage-gated Ca^{2+} entry was observed in fura-2-loaded GH_3 cells (a rat pituitary cell line) stimulated by high extracellular K^+, and in single smooth-muscle cells dissociated from rabbit ear artery held under voltage-clamp; in these smooth-muscle cells the effect of SK&F 96365 on ATP-evoked inward currents, via receptor-gated channels (Benham & Tsien, 1987), was also examined. We additionally looked at the inhibition by SK&F 96365 of functional responses, platelet aggregation and neutrophil adhesion and chemotaxis, under conditions where Ca^{2+} entry was expected to contribute to the activation process.

The effects of SK&F 96365 on platelets have been reported previously in a communication to the British Pharmacological Society (Merritt *et al.*, 1989*b*).

METHODS

Materials

Materials were obtained from the following sources: quin2 AM and Hepes (ultrapure) from Calbiochem; fura-2 AM from

Abbreviations used: $[Ca^{2+}]_i$, cytoplasmic free Ca^{2+} concentration; IC_{50}, concn. producing 50% inhibition; RMCE, receptor-mediated calcium entry; SK&F 96365, 1-{β-[3-(4-methoxyphenyl)propoxy]-4-methoxyphenethyl}-1*H*-imidazole hydrochloride; U46619, dideoxy-11α, 9α-epoxymethano-prostaglandin $F_{2\alpha}$.

* To whom correspondence and reprint requests should be addressed.

† Present address: Research Department, Ciba–Geigy Industrial Chemicals, Tenax Road, Trafford Park, Manchester M17 1WT, U.K.

‡ Present address: Glaxo Group Research Ltd., Greenford Road, Greenford, Middx. UB6 0HE, U.K.

§ Present address: Amylin Corporation, 9373 Towne Center Drive, Suite 250, San Diego, CA 92121, U.S.A.

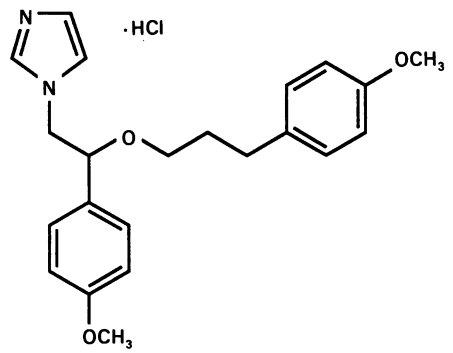

Fig. 1. Structure of SK&F 96365 (1-{β-[3-(4-methoxyphenyl)propoxy]-4-methoxyphenethyl}-1*H*-imidazole hydrochloride)

Molecular Probes Inc., Eugene, OR, U.S.A.; ADP and ATP from Boehringer; BSA, fibrinogen, digitonin, thrombin, fMet-Leu-Phe and histamine from Sigma; U46619 from The Upjohn Company, Kalamazoo, MI, U.S.A.

Synthesis of SK&F 96365

1-{β-[3-(4-Methoxyphenyl)propoxy]-4-methoxyphenethyl}-1*H*-imidazole hydrochloride (SK&F 96365; structure shown in Fig. 1) was synthesized by alkylation (KOH, dimethyl sulphoxide) of 1-(β-hydroxy-4-methoxyphenethyl)-1*H*-imidazole with 3-(4-methoxyphenyl)propanetoluene-*p*-sulphonate and subsequently converted into the hydrochloride with diethyl ether/HCl. The alcohol was prepared by $NaBH_4$ reduction of the known ketone, 1-(β-oxo-4-methoxyphenethyl)-1*H*-imidazole (Godefroi *et al.*, 1969). All compounds prepared exhibited analytical and spectroscopic data consistent with their structures.

Experiments with human platelets

Platelets were prepared from freshly drawn human blood as previously described (Pollock & Rink, 1986). For the experiments shown in Figs. 2 and 7, using quin2-loaded platelets, the platelet-rich plasma was incubated with 20 μM quin2 AM and 100 μM aspirin at 37 °C for 30 min. The platelets were then resuspended in medium containing NaCl (145 mM), KCl (5 mM), $MgCl_2$ (1 mM), $CaCl_2$ (0.2 mM), Hepes (10 mM, pH 7.4 at 37 °C), glucose (10 mM) and apyrase (10 μg/ml). $CaCl_2$ (1 mM) or EGTA (1 mM) was added as required. The platelets were incubated with SK&F 96365 for 2 min before stimulation with ADP, thrombin or U46619 to evoke rises in $[Ca^{2+}]_i$ (Fig. 2) or aggregation (Fig. 7). For measurement of $[Ca^{2+}]_i$ (Fig. 2), quin2 fluorescence was measured at 340 nm excitation, 500 nm emission in a Perkin–Elmer LS-5 fluorimeter at 37 °C.

Aggregation of quin-2-loaded platelets was monitored in a four-channel aggregometer (PAP-4 from Biodata Corp). Cells were prepared as above, but fibrinogen (1 mg/ml) was included in the medium and the cells were continuously stirred. The extent of aggregation was assessed 4 min after addition of the stimulus.

For the Mn^{2+} experiments, platelets were loaded with fura-2. Platelet-rich plasma was incubated with 2 μM fura-2 AM and 100 μM aspirin for 45 min. The platelets were then resuspended in medium containing 145 mM-NaCl, 5 mM-KCl, 1 mM-$MgCl_2$, 10 mM-Hepes (pH 7.4 at 37 °C), 10 mM-glucose and 10 μg of apyrase/ml. Fura-2 fluorescence was measured either in a Perkin–Elmer LS-5 fluorimeter at 500 nm emission and 360 nm excitation (Fig. 4*c*) or in a Spex dual-excitation-wavelength fluorimeter (Glen Creston Instruments, Stanmore, Middx., U.K.), at 500 nm emission and 340 and 360 nm excitation (Figs. 4*a* and 4*b*), as previously described (Sage *et al.*, 1989; Merritt *et al.*, 1989*a*).

Experiments with human neutrophils

Neutrophils were prepared from freshly drawn human blood by dextran sedimentation of erythrocytes followed by Percoll density-gradient centrifugation to separate leucocytes, as previously described (Merritt *et al.*, 1989*a*). The neutrophils were loaded with fura-2 by incubation for 30 min at 37 °C with 0.2 μM (for the experiments in Fig. 4) or for 45 min at 2 μM (for the experiments in Fig. 3) fura-2 AM in medium containing NaCl (145 mM), KCl (5 mM), $MgCl_2$ (1 mM), $CaCl_2$ (1 mM), Hepes (10 mM, pH 7.4 at 37 °C), glucose (10 mM) and BSA (1%). The neutrophils were then resuspended in the same medium but lacking fura-2 AM, $CaCl_2$ and BSA for measurement of fura-2 fluorescence. $CaCl_2$, EGTA or $MnCl_2$ were added as required. For the experiments shown in Fig. 3, fura-2 fluorescence was measured at 340 nm excitation, 500 nm emission in a Perkin–Elmer LS-5 fluorimeter at 37 °C. For the experiments shown in Fig. 4 (Mn^{2+} influx), fura-2 fluorescence was measured in a dual-excitation-wavelength Spex fluorimeter at 340 nm and 360 nm excitation, 500 nm emission (Merritt *et al.*, 1989*a*).

Adhesion of human neutrophils to plastic culture wells was measured as previously described (Davies *et al.*, 1990). Chemotaxis of neutrophils in response to fMet-Leu-Phe was measured by the 'under agarose' technique of Nelson *et al.* (1975).

Experiments with human umbilical-vein endothelial cells

Endothelial cells, obtained from human umbilical veins, were cultured on coverslips, loaded with fura2, and $[Ca^{2+}]_i$ was measured as previously described (Jacob, 1990). A coverslip was placed on the thermostatically regulated stage of an inverted microscope (Zeiss Axiomat) equipped with a ×40 (Nikon) fluorite objective, and the cells were superfused at 0.3 ml/min with medium containing 145 mM-NaCl, 5 mM-KCl, 1 mM-$CaCl_2$, 1 mM-$MgCl_2$, 10 mM-glucose, 0.1% BSA and 10 mM-Hepes (pH 7.4 at 37 °C). The cells were illuminated via the epi-fluorescence port of the microscope with excitation wavelengths of 350 nm and 380 nm, and the emitted light was detected by a photomultiplier. An autofluorescence correction was made at the end of each run by exposing the cells to 2 mM-$MnCl_2$ and 0.5 μM-ionomycin to quench the fura-2 fluorescence. $[Ca^{2+}]_i$ was calculated from the ratio of the fluorescence at the two excitation wavelengths (Grynkiewicz *et al.*, 1985).

Experiments with isolated smooth-muscle cells

Whole-cell recordings of voltage-gated Ca^{2+} currents or ATP-evoked currents in single smooth-muscle cells of rabbit ear artery were obtained as previously described (Benham & Tsien, 1987, 1988). Single freshly dissociated ear artery cells were held under voltage clamp by using standard patch-clamp techniques. A CsCl-based internal solution was used, and the external charge carrier was 110 mM-Ba^{2+} when voltage-gated Ca^{2+} currents were recorded (Benham & Tsien, 1988). Medium containing 130 mM-NaCl, 5 mM-KCl, 1.2 mM-$MgCl_2$, 1.5 mM-$CaCl_2$, 10 mM-glucose and 10 mM-Hepes (pH 7.2 at 22 °C) was used for experiments measuring the ATP-evoked current.

Analysis of data

Concentration/inhibition curves were fitted to the logistic equation by computer using the program ALLFIT (DeLean *et al.*, 1978).

RESULTS

Effects of SK&F 96365 on agonist-stimulated $[Ca^{2+}]_i$ responses in quin2-loaded human platelets

Fig. 2(*a*) shows typical fluorescence traces of quin2-loaded human platelets stimulated with ADP (20 μM) in the presence or

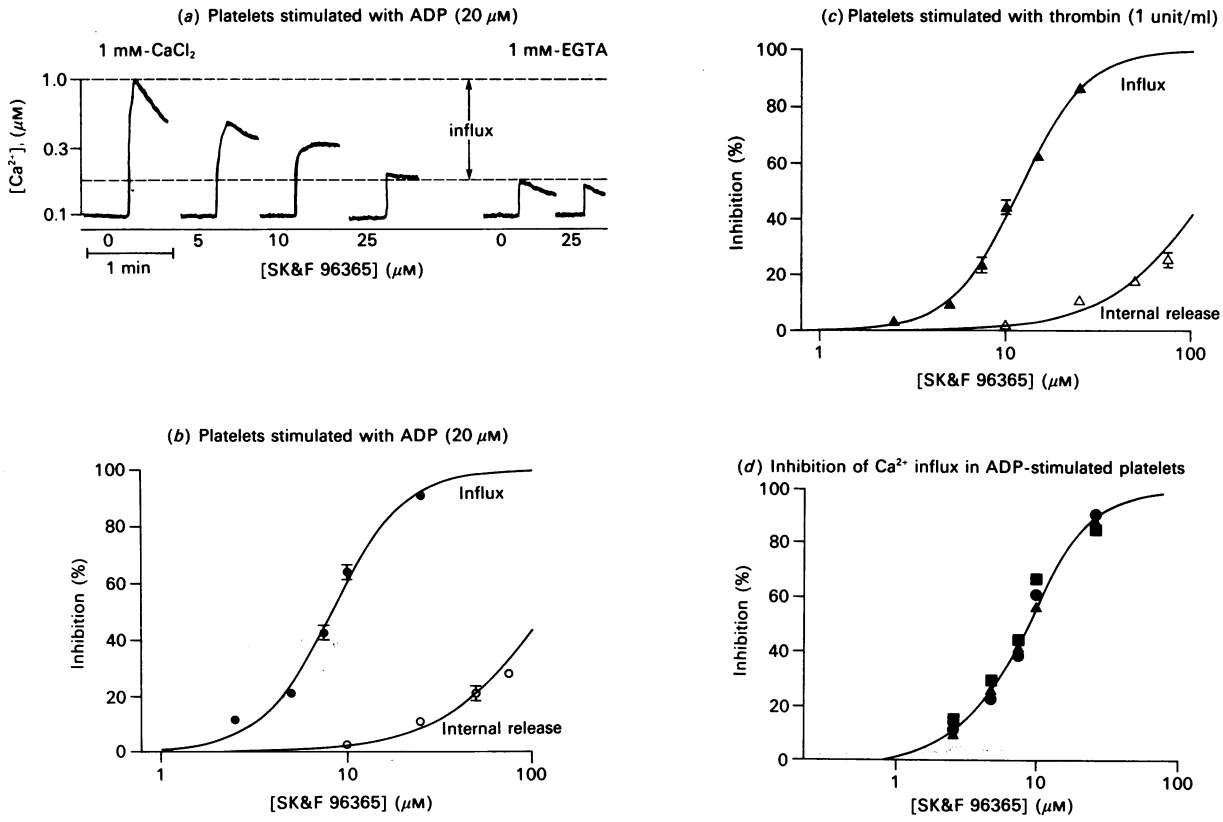

Fig. 2. Effect of SK&F 96365 on Ca^{2+} entry in quin2-loaded human platelets

(*a*) Typical raw fluorescence traces (with scale converted into $[Ca^{2+}]_i$) of quin2-loaded platelets stimulated with ADP (20 μM) in the presence or absence of external Ca^{2+} (1 mM-$CaCl_2$ or 1 mM-EGTA). SK&F 96365 (at the concentrations shown) was added 2 min before ADP. The difference in peak height of the control responses (with no added drug) measured in the presence or absence of external Ca^{2+} is attributed to Ca^{2+} influx. The controls contained dimethyl sulphoxide (0.1 %), which was the vehicle for the drug throughout. (*b*) Dose–response curves for inhibition by SK&F 96365 of both influx (●) and internal release (○) stimulated by ADP (20 μM). Percentage inhibition is calculated as inhibition of the fluorescence rise (measured in arbitrary fluorescence units) attributed to agonist-stimulated Ca^{2+} influx or internal release. Data are means ± S.E.M. of 3 experiments. Where not shown, the error bars are within the symbol size. (*c*) Dose–response curves for inhibition by SK&F 96365 of both influx (▲) and internal release (△) stimulated by thrombin (1 unit/ml). Data (from 3 experiments) were calculated and are represented as described above (Fig. 2*b*). (*d*) Dose–response curves for inhibition of ADP-evoked Ca^{2+} influx at three different $[Ca^{2+}]_o$: 0.2 mM (■), 1 mM (●) and 10 mM (▲). Data are means of 3 experiments; error bars (no greater than those shown in Figs. 2*b* and 2*c*) are omitted for clarity.

absence of external Ca^{2+}. This illustrates the protocol developed for assessing the ability of compounds to inhibit Ca^{2+} entry selectively, sparing internal Ca^{2+} release. For these experiments, platelets were relatively heavily loaded with quin2 to limit, in Ca^{2+}-free medium, the agonist-stimulated rise in $[Ca^{2+}]_i$ caused by the release of the finite pool of intracellular dischargeable Ca^{2+} (Pollock & Rink, 1986); in the presence of 1 mM external Ca^{2+}, agonist-stimulated Ca^{2+} entry from the essentially infinite extracellular source still allowed a large rise. The difference between the measured signals in the presence and absence of external Ca^{2+} is attributed to RMCE, and the ability of agents to decrease this difference can be expressed as percentage inhibition of RMCE. (This is only a semi-quantitative measure, since the rise in $[Ca^{2+}]_i$ is almost certainly not linearly dependent on Ca^{2+} influx.) In this example (Fig. 2*a*) 5–25 μM SK&F 96365 caused dose-dependent inhibition of the signal attributable to Ca^{2+} entry, with almost complete inhibition at 25 μM. By contrast, the final part of the trace shows that 25 μM SK&F 96365 caused very little decrease in the signal in Ca^{2+}-free medium and thus had much less effect on internal release. Fig. 2(*b*) shows the relation between SK&F 96365 concentration and inhibition of ADP-evoked Ca^{2+} entry and internal release. Percentage inhibition was calculated as inhibition of the fluorescence rise (measured in arbitrary fluorescence units) attributed to agonist-stimulated Ca^{2+} influx or release from intracellular stores. The IC_{50} for inhibition of ADP-stimulated Ca^{2+} entry by SK&F 96365 was 8.5 ± 0.4 μM, and the slope of the inhibition curve was 2.3 ± 0.3 ($n = 3$ experiments).

As expected for a functional antagonist, the inhibitory effect of SK&F 96365 is not specific for ADP; Fig. 2(*c*) shows a similar inhibition curve (IC_{50} = 11.7 ± 0.3 μM; slope = 2.4 ± 0.2; $n = 3$ experiments) for thrombin-stimulated Ca^{2+} entry. The effect of SK&F 96365 on internal release evoked by ADP or thrombin was only small (≈ 10 % inhibition at a concentration that causes 90 % inhibition of entry). Similar results were also seen when $[Ca^{2+}]_i$ was elevated by using the thromboxane mimetic U46619 (not shown).

Under certain experimental conditions, such as contraction of K^+-depolarized muscle by re-admission of various concentrations of external Ca^{2+} ($[Ca^{2+}]_o$), the 'classic' calcium antagonists such as nifedipine or verapamil show apparent competition with $[Ca^{2+}]_o$; the $[Ca^{2+}]_o$-response curves are shifted to the right (see, e.g., Spedding, 1982). We therefore tested SK&F 96365 on ADP-evoked responses at three different $[Ca^{2+}]_o$, 0.2, 1.0 and 10.0 mM. Fig. 2(*d*) shows that the inhibition curves were almost superimposable, with IC_{50} values of 8.0 ± 0.6, 8.5 ± 0.4 and 8.8 ± 0.3 μM respectively ($n = 3$ separate experiments). This result indicates a lack of competition between Ca^{2+} and SK&F 96365.

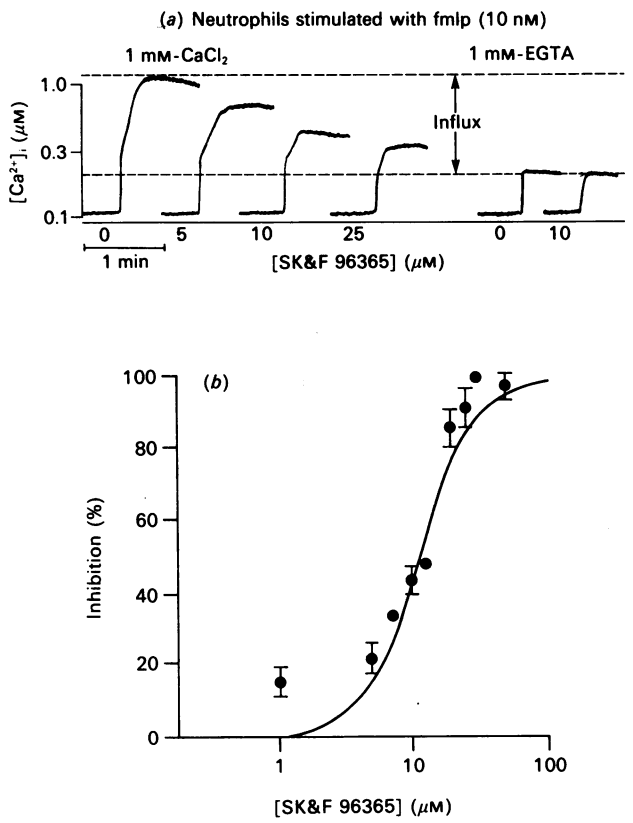

Fig. 3. Effect of SK&F 96365 on Ca^{2+} entry in fura-2-loaded human neutrophils

(*a*) Typical fluorescence traces, with scale converted into $[Ca^{2+}]_i$, of fura-2-loaded neutrophils stimulated with fMet-Leu-Phe (fmlp, 10 nM) in the presence or absence of external Ca^{2+} (1 mM-$CaCl_2$ or 1 mM-EGTA). SK&F 96365 was added (at the concentrations shown) 2 min before fMet-Leu-Phe. (*b*) Dose–response curve for inhibition by SK&F 96365 of Ca^{2+} influx stimulated by fMet-Leu-Phe (10 nM). Percentage inhibition was calculated as described for platelets (Fig. 2). Data are means ± S.E.M. of 3–7 experiments (where not shown, the error bars are within the symbol size).

Effects of SK&F 96365 on $[Ca^{2+}]_i$ responses of fura-2-loaded human neutrophils

Experiments with fura-2-loaded neutrophils showed that SK&F 96365 could inhibit RMCE in a different cell type. Human neutrophils were heavily loaded with fura-2 (2 μM fura-2 AM for 45 min at 37 °C, giving a cytosolic fura-2 concentration of approx. 0.5 mM) to buffer changes in $[Ca^{2+}]_i$ and allow a measure of Ca^{2+} influx similar to that described above for platelets. Fig. 3(*a*) shows typical fluorescence traces of fura-2-loaded neutrophils stimulated with fMet-Leu-Phe (10 nM) in the presence or absence of external Ca^{2+}, and in the presence of SK&F 96365. As with platelets, it is apparent that a concentration of SK&F 96365 (10 μM) which causes approx. 50% inhibition of Ca^{2+} influx has little or no effect on internal release; some inhibition is observed at higher concentrations. SK&F 96365 was added to the neutrophils 2 min before fMet-Leu-Phe. Fig. 3(*b*) shows a dose–response curve for inhibition of fMet-Leu-Phe-stimulated Ca^{2+} influx in fura-2-loaded neutrophils. The IC_{50} for SK&F 96365 was 11.2 ± 1.4 μM and the slope was 2.2 ± 0.4 ($n = 7$ separate experiments). Platelet-activating-factor-stimulated Ca^{2+} influx was also inhibited by similar concentrations of SK&F 96365 (results not shown).

Effects of SK&F 96365 on Mn^{2+} entry in platelets and neutrophils

We have interpreted the results in Figs. 2 and 3 as showing inhibition of RMCE, but an alternative explanation could be that the rise in $[Ca^{2+}]_i$ is decreased by SK&F 96365, owing to enhancement of Ca^{2+} extrusion. This is perhaps unlikely, in view of the weak effects on internal release, where an enhanced efflux should also decrease the response. More importantly, analysis of Mn^{2+} entry (Merritt *et al.*, 1989*a*; Sage *et al.*, 1989), where responses can be more definitely attributed to influx, supports our interpretation. Mn^{2+} influx, through bivalent-cation-permeable channels, is readily detected because Mn^{2+} binds with high affinity to fura-2 and powerfully quenches the fluorescence signal at all excitation wavelengths, including the isoemissive wavelength (360 nm). Fig. 4 shows the use of this technique to distinguish internal Ca^{2+} release and Mn^{2+} entry in thrombin-stimulated fura-2-loaded platelets (Fig. 4*a*) and in fMet-Leu-Phe-stimulated fura-2-loaded neutrophils (Fig. 4*b*). Both the platelets and the neutrophils were lightly loaded with fura-2 to a cytosolic concentration of 50–100 μM. The upper pairs of traces in both Figs. 4(*a*) and 4(*b*) show control responses. The 340 nm signal (continuous line) shows first the abrupt rise in fluorescence owing to agonist-evoked release of intracellular Ca^{2+} stores. After this, both traces are quenched, reflecting Mn^{2+} entry; this is more clearly seen on the 360 nm trace. The upper traces in Fig. 4(*a*) (platelets) also show little further quenching when the cells were permeabilized with digitonin. The effect of SK&F 96365 (30 μM on platelets and 10 μM on neutrophils) is shown in the lower pairs of traces. The internal release, detected at the 340 nm excitation wavelength, is essentially unchanged; the Mn^{2+} entry is markedly decreased. Fig. 4(*c*) shows dose–response curves for inhibition of Mn^{2+} influx into platelets stimulated with ADP (40 μM), thrombin (1 unit/ml) or U46619 (1 μM). The IC_{50} values for inhibition by SK&F 96365 were 22.5 ± 1.4, 27.4 ± 1.6 and 17.8 ± 1.9 μM respectively. The fMet-Leu-Phe-stimulated Mn^{2+} entry into fura-2-loaded neutrophils was almost completely inhibited by 10 μM SK&F 96365. Similar results were obtained with ATP-stimulated Mn^{2+} entry in neutrophils (results not shown).

In these experiments where platelets and neutrophils were only lightly loaded with fura-2, SK&F 96365 (at high concentrations) itself sometimes caused a transient elevation in $[Ca^{2+}]_i$. Fig. 4(*a*) also shows a small increase in $[Ca^{2+}]_i$ evoked by 30 μM SK&F 96365 in platelets. This effect of SK&F 96365 was most noticeable with fura-2-loaded neutrophils; 20 μM SK&F 96365, which inhibited Ca^{2+} influx by 88 ± 6%, caused a transient increase in $[Ca^{2+}]_i$ of 100–200 nM. Further investigation revealed that this was due to release of Ca^{2+} from internal stores; the response was observed in the absence of external Ca^{2+}, and SK&F 96365 did not cause Mn^{2+} entry (similar effects were occasionally seen with endothelial cells). When the effects of SK&F 96365 were examined on $InsP_3$-releasable Ca^{2+} stores in saponin-permeabilized rat hepatocytes, at concentrations of 30 μM and above, the compound caused the release of Ca^{2+}; there was no inhibition of $InsP_3$-induced Ca^{2+} release (C. W. Taylor, personal communication). Thus it is important to note that SK&F 96365 can have additional effects which require investigation in each preparation.

Effects of SK&F 96365 on single superfused fura-2-loaded human umbilical-vein endothelial cells

Endothelial cells are a further example of a non-excitable cell where RMCE has an important role in Ca^{2+} signalling (Hamilton & Sim, 1987; Jacob *et al.*, 1988; Jacob, 1990). Fig. 5 illustrates three examples of effects of SK&F 96365 on Ca^{2+} entry in single

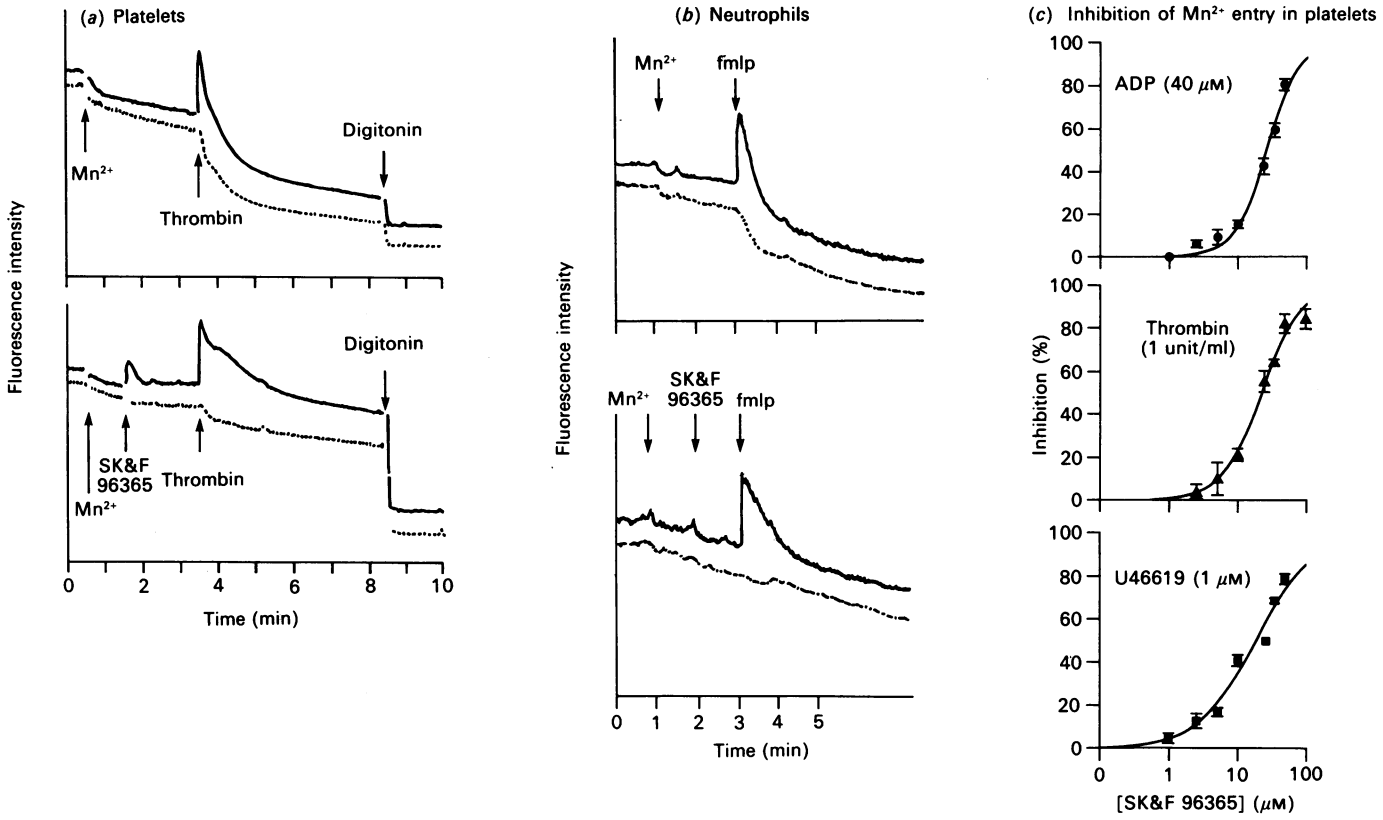

Fig. 4. Effect of SK&F 96365 on stimulated Mn^{2+} influx into fura-2-loaded platelets and neutrophils

(*a*) Thrombin-stimulated Mn^{2+} influx into fura-2-loaded human platelets. Raw fluorescence traces are shown (emission 500 nm) with excitation at 340 nm (——) and 360 nm (----). Fura-2 fluorescence at 340 nm excitation increases with increasing $[Ca^{2+}]_i$, and Mn^{2+} entry quenches the signal. At 360 nm excitation (the isoemissive wavelength) the signal is independent of $[Ca^{2+}]_i$, but is still quenched by Mn^{2+}. The following additions were made at the times shown: $MnCl_2$ (Mn^{2+}; 100 μM), thrombin (1 unit/ml), SK&F 96365 (30 μM) and digitonin (15 μM). (*b*) fMet-Leu-Phe-stimulated Mn^{2+} influx into fura-2-loaded human neutrophils. The protocol was similar to that described above (Fig. 4*a*), with the following additions at the times shown: $MnCl_2$ (Mn^{2+}; 100 μM), fMet-Leu-Phe (fmlp; 10 nM), SK&F 96365 (10 μM). (*c*) Dose–response curves for inhibition by SK&F 96365 of Mn^{2+} entry stimulated by 40 μM-ADP (●; top panel), 1 unit of thrombin/ml (▲; middle panel) and 1 μM-U46619 (■; bottom panel). Inhibition of Mn^{2+} entry was measured as inhibition of the extent of quenching of fluorescence at 360 nm excitation. Data are means ± S.E.M. of 3 experiments. Where not shown, the error bars are within the symbol size.

fura-2-loaded endothelial cells dissociated from human umbilical vein. An important point seen with these superfused preparations is the relatively rapid onset of action and ready reversibility of the effects of SK&F 96365. In Fig. 5(*a*), the first two histamine responses show the patterns seen with a supramaximal concentration of histamine (100 μM) in the presence and absence of external Ca^{2+}. In the presence of Ca^{2+}, the response consists of the typical early $[Ca^{2+}]_i$ peak and the secondary plateau phase attributed to RMCE; in the absence of external Ca^{2+}, the plateau phase is absent. The next histamine response, in the presence of 1 mM-Ca^{2+} and 30 μM SK&F 96365, was similar to that seen in the absence of external Ca^{2+}, consistent with selective blockade of histamine-evoked RMCE and sparing of internal release. Reversibility of the effect of SK&F 96365 was indicated by the increase in $[Ca^{2+}]_i$ to the expected plateau level after removal of SK&F 96365. Finally, a fourth histamine response in the presence of 1 mM-Ca^{2+} was similar to the initial control.

Fig. 5(*b*) shows the sequential application and removal of successively higher concentrations of SK&F 96365 after establishment of a plateau phase in the presence of 100 μM-histamine and 1 mM-$CaCl_2$. In this example, the IC_{50} for RMCE was approx. 10 μM. Fig. 5(*c*) illustrates another effect sometimes seen with SK&F 96365. Here, an endothelial cell has been stimulated with a low concentration of histamine (0.5 μM) to set up a train of $[Ca^{2+}]_i$ spikes (Jacob *et al.*, 1988). Application of 30 μM SK&F 96365 then abruptly terminated the spikes and left $[Ca^{2+}]_i$ at the basal level. On removal of the SK&F 96365, spiking restarted. The result points to a significant role for Ca^{2+} entry in maintaining the sequence of Ca^{2+} oscillations.

Effects of SK&F 96365 on voltage-gated Ca^{2+} entry

The results described so far show that SK&F 96365 can selectively block RMCE in three types of non-excitable cells. In two different excitable cells, we found that the compound also inhibits voltage-gated Ca^{2+} entry. In fura-2-loaded GH_3 cells, elevation of $[Ca^{2+}]_i$ by 50 mM-K^+ or 50–100 nM-(−) BayK 8644 (an agonist for L-type Ca^{2+} channels) was dose-dependently decreased by SK&F 96365, with an IC_{50} of 3.6 μM.

Fig. 6 shows the effect of SK&F 96365 on the Ba^{2+} current through L-type voltage-gated Ca^{2+} channels in single smooth-muscle cells dissociated from rabbit ear artery. The current was measured by whole-cell patch-clamp and evoked by a voltage step from −80 mV to +30 mV (Benham & Tsien, 1988). Fig. 6(*a*) shows the control current compared with that evoked in the presence of SK&F 96365 (50 μM), and Fig. 6(*b*) shows the cumulative effect of increasing concentrations of SK&F 96365 on this current. In four experiments, the IC_{50} against this dihydropyridine-sensitive Ca^{2+} current was 20–30 μM. Fig. 6(*b*)

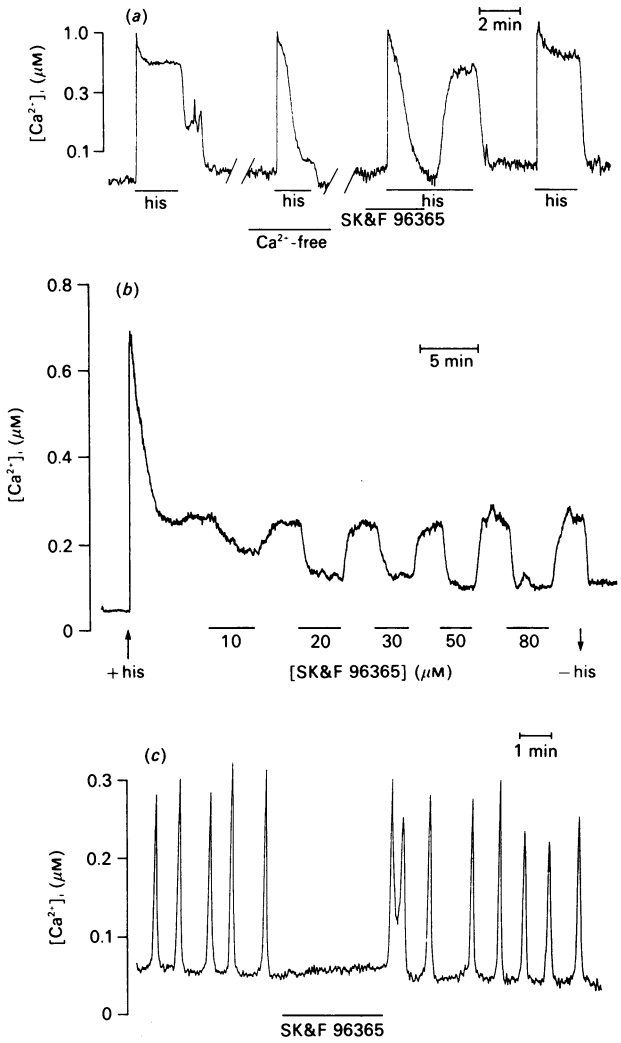

Fig. 5. Effect of SK&F 96365 on single human umbilical-vein endothelial cells stimulated with histamine

(*a*) A single endothelial cell was continuously superfused with medium containing 1 mM-$CaCl_2$ unless otherwise indicated. The bars indicate the time during which the superfusate contained histamine (his; 100 μM), SK&F 96365 (30 μM) or lacked $CaCl_2$ (Ca^{2+}-free). (*b*) A single cell was superfused with Ca^{2+}-containing medium and was exposed to histamine (100 μM) throughout the times between the arrows labelled as '+his' and '−his'. The bars show the times during which the cell was exposed to SK&F 96365 at the concentrations (μM) indicated. (*c*) A single cell was superfused with medium containing 1 mM-$CaCl_2$ and histamine (0.5 μM). The cell was exposed to SK&F 96365 (30 μM) during the time indicated by the bar.

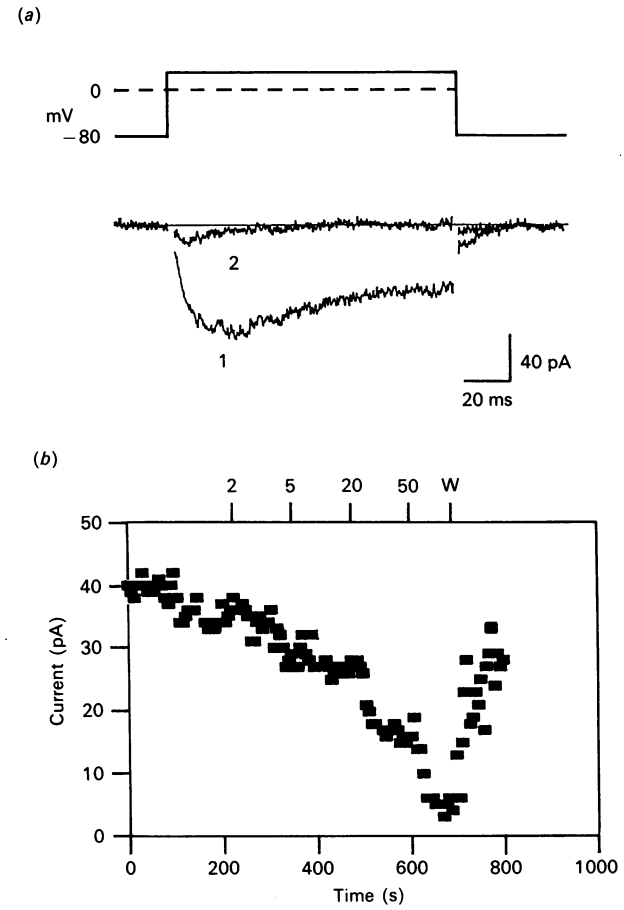

Fig. 6. Effect of SK&F 96365 on Ca^{2+}-channel currents in single patch-clamped vascular smooth-muscle cells from rabbit ear artery

(*a*) Effect of SK&F 96365 (50 μM) on Ca^{2+}-channel evoked by depolarization to +30 mV from −80 mV. Trace 1 is the control current and trace 2 is the current 1 min after application of SK&F 96365 (50 μM). (*b*) Plot of peak Ca^{2+}-channel current measured at +30 mV every 12 s to show effect of cumulative additions of SK&F 96365. The vertical lines indicate times of drug addition, and the numbers are the concentrations (μM) of SK&F 96365: W indicates wash-out of the drug.

also illustrates the reversibility of the inhibition by SK&F 96365; when the compound was washed out, the Ca^{2+} current was restored rapidly. The ATP-receptor-gated current evoked in this preparation by 10 μM-ATP at −60 mV (Benham & Tsien, 1987) was unaffected by 20 μM SK&F 96365; the control response was 7.2 ± 1.3 pA/pF ($n = 6$) and that in the presence of SK&F 96365 was 9.1 ± 1.1 pA/pF ($n = 7$). As the ATP-gated current desensitizes rapidly, this experiment was performed on 13 cells from the same preparation.

Inhibition by SK&F 96365 of aggregation of quin2-loaded platelets

Having shown that SK&F 96365 can inhibit RMCE in human platelets, neutrophils and endothelial cells (Figs. 2–5), we next used SK&F 96365 to see whether this inhibition might be of functional importance in platelets. In cells that are loaded with quin2, SK&F 96365 clearly limits the extent of $[Ca^{2+}]_i$ rise (Fig. 2*a*) and might be expected to decrease a functional response dependent on Ca^{2+}-activated processes. Fig. 7 shows studies of aggregation of platelets; Fig. 7(*a*) shows aggregation traces for quin2-loaded platelets stimulated with the thromboxane mimetic U46619 (1 μM) in the presence of various concentrations of SK&F 96365. Under these conditions, there was no aggregation in the absence of extracellular Ca^{2+}. Fig. 7(*b*) shows the dose–response curve for inhibition of platelet aggregation by SK&F 96365. The IC_{50} for SK&F 96365 was 15.9 ± 0.7 μM (slope = 1.8 ± 0.1; $n = 3$ experiments). This value is similar to that for inhibition of RMCE. In an extension of this analysis, comparing inhibition of RMCE and of aggregation with a series of novel compounds, we found a correlation between the measured IC_{50} values for these two variables (Armstrong *et al.*, 1989).

When tested, under the same conditions, on platelets that were not loaded with quin2, SK&F 96365 did not inhibit aggregation, presumably because in these cells the $[Ca^{2+}]_i$ rise owing to internal release can exceed 1 μM (Pollock & Rink, 1986), which is

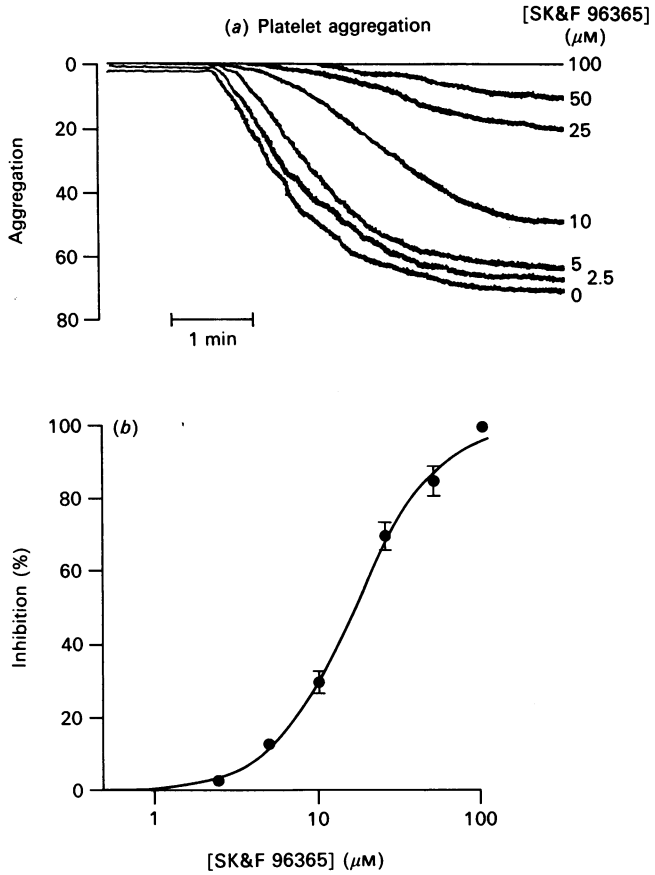

Fig. 7. Effect of SK&F 96365 on aggregation of quin2-loaded human platelets

(*a*) Typical aggregation traces showing U46619 (1 μM)-stimulated aggregation of platelets in the presence of various concentrations of SK&F 96365 (added 2 min before U46619). (*b*) Dose–response curve for inhibition by SK&F 96365 of aggregation stimulated by U46619 (1μM). Percentage inhibition is calculated as inhibition of the maximal extent of aggregation. Data are means ± S.E.M. of 3 experiments (where not shown the error bars are within the symbol size).

sufficient to trigger the functional response. This result also shows that SK&F 96365 does not inhibit other processes required for aggregation.

Inhibition of neutrophil adhesion and chemotaxis by SK&F 96365

Experiments with human neutrophils have shown a partial dependence of adhesion and chemotaxis on extracellular Ca^{2+} and Ca^{2+} entry (Davies *et al.*, 1990; J. E. Merritt, unpublished work). SK&F 96365 decreased both adhesion and the chemotaxis evoked by fMet-Leu-Phe in the presence of extracellular Ca^{2+}; the maximum decrease in both adhesion and chemotaxis seen with SK&F 96365 was similar to that seen in Ca^{2+}-free medium. Adhesion of fMet-Leu-Phe-stimulated neutrophils in the presence of SK&F 96365 (30 μM) was 55% of the fMet-Leu-Phe-stimulated control, and the response in the absence of extracellular Ca^{2+} was 54% of control. The IC_{50} for inhibition of adhesion by SK&F 96365 was in the range 5–10 μM. Chemotaxis of fMet-Leu-Phe-stimulated neutrophils in the presence of SK&F 96365 (30 μM) was 42 ± 3% ($n = 6$) of the fMet-Leu-Phe-stimulated control, and the response in the absence of extracellular Ca^{2+} was 51 ± 11% ($n = 3$) of control.

Since SK&F 96365 decreases Ca^{2+} entry in both neutrophils and endothelial cells, it might be expected to have anti-inflammatory or anti-oedema properties. In preliminary tests we found that intradermal injection of 50 nmol of SK&F 96365 partially inhibited the extravasation of ^{125}I-albumin and Evans Blue dye induced by intradermal injection of histamine plus prostaglandin E_2 in anaesthetized rabbits. The response in the presence of SK&F 96365 (50 nmol) was 80 ± 4% ($n = 4$) of the control response.

DISCUSSION

The results presented here show that SK&F 96365 can selectively decrease RMCE in human platelets, neutrophils and endothelial cells, while sparing receptor-evoked internal Ca^{2+} discharge. This action was revealed by using either the stimulus-evoked rise in $[Ca^{2+}]_i$ that was dependent on external Ca^{2+}, or Mn^{2+} entry, as an index of Ca^{2+} entry. The IC_{50} for the inhibitory effects was in the range of 10–20 μM for several different agonists, and for several cell types, showing that SK&F 96365 acted as a 'functional' antagonist and not on specific receptors. The lack of effect on internal Ca^{2+} release at these concentrations indicates selectivity for inhibition of Ca^{2+} entry and relative sparing of other signal-transduction processes. At higher concentrations, there were effects on internal Ca^{2+} release; some inhibition was observed (see, e.g., Figs. 2*b* and 2*c*), and in some conditions in either intact or permeabilized cells SK&F 96365 appeared to cause some discharge of intracellular Ca^{2+} stores.

SK&F 96365 blocks Ca^{2+} entry or currents via L-type voltage-gated Ca^{2+} channels in the two cells types tested (GH_3 cells and arterial smooth-muscle cells) at least as potently as it decreases RMCE. This property will be distinctly disadvantageous in attempts to analyse Ca^{2+} entry in excitable cells, but may not matter unduly with non-excitable cells, such as platelets, neutrophils and endothelial cells. Clearly investigators wishing to work with the new compound must exercise due caution in designing and interpreting their experiments.

SK&F 96365 had little effect on ATP-gated channels in arterial smooth-muscle cells. This result demonstrates that the compound does not cause general inhibition of channels simply by its presence in the membrane, which might have been the case for this very hydrophobic compound. This result also shows that the ATP-gated channel of smooth muscle is distinctly different from the RMCE mechanisms in the other cells examined, including the ADP-gated channel in platelets, which, as shown by our data and those of Sage *et al.* (1990), is blocked by SK&F 96365. It may be that this compound is specific for channels that are highly selective for Ca^{2+}, such that the less Ca^{2+}-selective ATP-gated channel is not blocked.

Another potentially useful feature is the ready reversibility of the effect of SK&F 96365 seen in the experiments with single endothelial and smooth-muscle cells, where the superfusate could be readily switched from drug-containing to drug-free medium.

The action of SK&F 96365 in decreasing the plateau phase of a histamine-evoked maximal $[Ca^{2+}]_i$ response in endothelial cells fits well with its effects in platelets and neutrophils. The effects of SK&F 96365 on the $[Ca^{2+}]_i$ spikes evoked by low concentrations of histamine are intriguing. We have shown that removal of external Ca^{2+} stops a train of spikes, but usually after two or three slower and smaller transients (Jacob *et al.*, 1988). We do not know why SK&F 96365 can immediately and reversibly abrogate spiking as in Fig. 5(*c*). It is clear that Ca^{2+} entry plays no part in the main part of spike generation, since removal of external Ca^{2+} just before a spike occurs has no measurable effect on the rapidly rising phase or peak height (Jacob *et al.*, 1988). But from the effects of Ca^{2+} removal and of SK&F 96365, we

must assume that maintaining spiking in endothelial cells requires some form of RMCE.

The main purpose of this study was to investigate the actions of SK&F 96365 on RMCE to elucidate the behaviour of the compound and gain insights into the mechanisms of RMCE. Equally important was examining the functional significance of RMCE in cell activation and the possible utility of blockers of RMCE in disease states, particularly those that may arise from multi-mediator pathology. Our preliminary results on platelet aggregation and neutrophil adhesion and chemotaxis show that SK&F 96365 does have the expected inhibitory effects under conditions where the functional responses are known to be dependent on RMCE. The effect of SK&F 96365 on aggregation of quin2-loaded platelets is consistent with an important role for RMCE in aggregation under these conditions, and gives an indication of the $[Ca^{2+}]_i$-dependence of membrane events of aggregation, namely the conformational change of glycoproteins IIb/IIIa that constitute the fibrinogen receptor. This analysis would be difficult when using low external $[Ca^{2+}]$ or cations such as Ni^{2+} or La^{3+} to inhibit Ca^{2+} entry, since the behaviour of the fibrinogen receptor, and fibrinogen binding, is markedly affected by bivalent-cation concentration (see, e.g., Seiss, 1989). Under conditions where the functional responses are not dependent on RMCE, as expected SK&F 96365 has no inhibitory effect; this is an important result, showing that the compound is selective for inhibition of RMCE and that it does not inhibit other cellular responses.

In conclusion, we have identified a novel compound which can selectively decrease RMCE in platelets, neutrophils and endothelial cells while sparing receptor-mediated internal Ca^{2+} discharge. The lack of effect on the ATP-activated channel in smooth muscle points to some selectivity in the action of this compound between different types of RMCE. SK&F 96365 inhibits RMCE evoked by each of the agonists tested in human platelets, neutrophils and endothelial cells. The selectivity of RMCE over internal discharge is only relative, and should be checked on each preparation. A property that we would like to 'design out' of subsequent structures is a significant blockade of voltage-gated Ca^{2+} channels. However, SK&F 96365 should prove to be a valuable tool for probing of receptor-mediated Ca^{2+} entry processes, particularly in non-excitable cells. It may also have use *in vivo* where the requisite manipulations of external Ca^{2+} or application of transition metals such as Mn^{2+}, Ni^{2+} or La^{3+} to probe RMCE are not readily feasible. The possibility that blockade of receptor-mediated calcium entry will have therapeutic utility in disease states dependent on multi-mediator overactivity remains to be tested.

Received 14 May 1990/11 June 1990; accepted 26 June 1990

S.A.McC. was an extramural student from King's College, London (Department of Biochemistry). We thank Ms. S. Luker for secretarial assistance, Dr. S. Sage for discussion, and Dr. J. D. Pearson, M.R.C. Clinical Research Centre, Harrow, for providing the endothelial cells.

REFERENCES

Armstrong, W. P., Cassidy, K., Dolle, R. E., Howson, W., Jaxa-Chamiec, A., Novelli, R., Tchorzewska, M. A., Hallam, T. J., Leigh, B. K., Merritt, J. E., Moores, K. E. & Rink, T. J. (1989) in Ion Transport (Benham, C. D. & Keeling, D. J., eds.), pp. 336–337, Academic Press, London

Benham, C. D. & Tsien, R. W. (1987) Nature (London) **328**, 275–278

Benham, C. D. & Tsien, R. W. (1988) J. Physiol. (London) **404**, 767–784

Berridge, M. J. (1988) Proc. R. Soc. London Ser. B **234**, 359–378

Campbell, K. P., Leung, A. T. & Sharp, A. H. (1988) Trends Neurosci. **11**, 425–430

Cobbold, P. H. & Rink, T. J. (1987) Biochem. J. **248**, 313–328

Davies, M. P. A., Hallam, T. J. & Merritt, J. E. (1990) Biochem. J. **267**, 13–16

DeLean, A., Munson, P. J. & Rodbard, D. (1978) Am. J. Physiol. **253**, E97–E102

Godefroi, E. F., Heres, J., Vancutsem, J. & Janssen, P. A. (1969) J. Med. Chem. **12**, 784–791

Grynkiewicz, G., Poenie, M. & Tsien, R. Y. (1985) J. Biol. Chem. **260**, 3440–3450

Hallam, T. J. & Rink, T. J. (1985) FEBS Lett. **186**, 175–179

Hallam, T. J. & Rink, T. J. (1989) Trends Pharmacol. Sci. **10**, 8–10

Hamilton, K. K., & Sim, P. J. (1987) J. Clin. Invest. **79**, 600–668

Jacob, R. (1990) J. Physiol. (London). **421**, 55–77

Jacob, R., Merritt, J. E., Hallam, T. J. & Rink, T. J. (1988) Nature (London). **335**, 40–45

Meldolesi, J. & Pozzan, T. (1987) Exp. Cell Res. **171**, 271–272

Merritt, J. E., Jacob, R. & Hallam, T. J. (1989*a*) J. Biol. Chem. **264**, 1522–1527

Merritt, J. E., Armstrong, W. P., Hallam, T. J., Jaxa-Chamiec, A., Leigh, B. K., Moores, K. E. & Rink, T. J. (1989*b*) Br. J. Pharmacol. **98**, 674*P*

Nelson, R. D., Quie, P. G. & Simmons, R. L. (1975) J. Immunol. **115**, 1650–1656

Pollock, W. K. & Rink, T. J. (1986) Biochem. Biophys. Res. Commun. **139**, 308–314

Putney, J. W. (1987) Trends Pharmacol. Sci. **8**, 481–486

Ross, C. A., Meldolesi, J., Milner, T. A., Satoh, T., Supattapone, S. & Snyder, S. H. (1989) Nature (London). **339**, 468–471

Sage, S. O., Merritt, J. E., Hallam, T. J. & Rink, T. J. (1989) Biochem. J. **258**, 923–926

Sage, S. O., Reast, R. & Rink, T. J. (1990) Biochem. J. **265**, 675–680

Seiss, W. (1989) Physiol. Rev. **69**, 58–178

Spedding, M. J. (1982) Naunyn-Schmiedeberg's Arch. Pharmacol. **318**, 234–240

Tsien, R. W., Lipscombe, D., Madison, D. V., Bley, K. R., & Fox, A. P. (1988) Trends Neurosci. **11**, 431–438